Optimal operation of building microgrids - comparison with mixed-integer linear and continuous non-linear programming approaches

Vincent Reinbold, Van-Binh Dinh, Daniel Tenfen, Benoît Delinchant, Dirk Saelens

DRAFT

Optimal Operation of Building Microgrids - Comparison for Mixed-Interger Linear and Continuous Non-Linear

Vincent REINBOLD*, Van-Binh DINH†, Daniel TENFEN‡, Benoit DELINCHANT†, Dirk SAELENS*

*KU Leuven - University of Leuven, Department of Civil Engineering, 3001 Leuven, Belgium, E-mail: vincent.reinbold@kuleuven.be

†Grenoble University, G2eLab (CNRS UMR5269, INPG, UJF), F-38142 Cedex, Grenoble, France

‡IFSC - Av. Mauro Ramos, 950, Centro - DAE, Florianópolis - CEP 88020-300

Abstract. This paper presents two mathematical models for the load demand to the Energy Management (EM) problem of a Micro-Grid (MG), by means of deterministic Mixed Integer Linear Programming (MILP) and Non-Linear Programming (NLP) approaches. A general architecture of a microgrids is proposed, involving Energy Storage Systems (ESS), Distributed Generation (DG) and a thermal reduced-model of the grid-connected dwelling. It focuses on the modelling process and the optimization performances for both approaches regarding optimal operation of near zero energy buildings related to electric microgrid within a time horizon of 24 hours.

Keywords. optimal operation, zero energy buildings, micro-grid, MILP, SQP

1. Introduction

1.1 Background and Motivation

Building operation is an important topic in order to contribute to consumptions reduction and energy grid interaction. Demand response in electricity market has already been addressed by the research community [1]. According to local constraints of energy delivery, the optimal control of grid-connected and standalone nearly/net zero energy buildings must be addressed [2]. In this paper, we are investigating the optimal operation of the smart building regarding weather forecast, local renewable energy production and grid prices. The Energy Management Problem (EMP), *i.e.* optimization algorithm associated with predictive models and criteria, may have different nature. We will focus on the influence of linear or non-linear formulation and optimization performances.

1.2 Literature Review

1.2.1 Microgrid Energy Management

The demand response and demand side management concepts are a trend that is currently in progress in the modern electric energy industry [1,3–5]. The controllable loads might reduce fossil fuel consumption, load peak shaving, as well as postpone investments in new transmission and distribution lines if successfully implemented. Also, in the modern electric energy industry, the microgrids (MGs) are emerging as an additional element to maintain the growth and sustainability [6]. Microgrid's EMP, also known as scheduling problem, aims to minimize, the operation costs of DERs, as well as the power exchange with the main grid [6, 7]. In the paper, we choose a centralized approach to ensure global optimality and a smart management of electrical and thermal storages.

1.2.2 Thermal Load Management

Demand side management (DSM) in the electricity grid usually involves energy efficiency and demand response (DR). Numerous studies has been devoted to promote load shifting, efficient energy technologies or even energy awareness. In [8], Palensky et al. propose an overview of DSM, including Demad Response (DR). For thermal demand side management, several studies reach significant savings using multi-agent based [9] or integrated centralized approaches coupled with thermal storage [10, 11]. In microgrids' literature, thermal demand side management is not usually introduced in the electrical modelling. As a new approach, we consider the smart-building as a MG unit, subjected to comfort and air quality criteria. A Direct Load Control on the forced-air heating system of the Smart-Building is considered as the thermal mass of the building could be used for storage.

1.2.3 MILP vs. NLP formulation

The difference between linear and non-linear formulation is related to the nature of constraints and objective functions. In the case of MILP formulations, mixed continuous-discrete are usually artificially introduced in the modelling stage to overcome non-linearities. In addition, it often introduces approximations and may leads to different modelling, which make the comparison difficult [12]. This approximation stage is tedious and error prone. One possible solution is to automate this transformation from a physical model into MILP suited model using Model Driven Engineering (MDE). It usually leads to different nature of decision variables which are kept continues in the case of non-linear and are mixed continuous-discrete in the case of MILP formulations. One of the main techniques are based on discretization, piecewise approximation or Taylor series expansions in order to be compatible with MILP algorithm. The main drawbacks of NLP are the continuous definition set and convergence properties, indeed, the global convergence is guarantee only for convex cases (convex objective function and inequality constraints).

1.3 Contribution

Novel contributions of this work include:

- Introduction and formulation of the Thermostatically Controlled Loads (TCL) within the microgrid. The resulting Linear Program handles the mutli-objective trade-off between discomfort and cost of use taking into account air quality criterion.
- Linearisation and formulation of the ventilation system behaviour. Which is generally non-linear and non-convex equality constraints, involving air quality model, heat transfer, and ventilation power.
- Comparison of both MILP and NLP methods on a general use case which provides a solution that can be interpreted for implementation.

1.4 Paper Outline

This paper is organized as follows. Section 2. describes the general optimization problem and presented both, NLP and MILP, formulations. It describes the models and the linearisation techniques for each involved physic (e.g. electrical, thermal and ventilation). Section 3. provides a computational example where the building structure and electrical units are described. Results' analysis are performed in section 4. Finally, section 5. summarizes keys results.

2. General Formulation and Linearisation

In the paper, the EM optimization is related to the physical and economical framework in which the MG is inserted. The smart building involves a thermal envelope, an ideal heating system and a general ventilation system (with or without heat recovery). It is connected to the MG which consists of a battery pack, photovoltaic panels and a connection to the main grid. The system is subjected to forecasts such as occupancy, solar irradiation, external temperature and energy prices.

This section is organized by field: electric, thermal and ventilation models will be detailed. For each physic, both NLP and MILP are formulation and differences will be highlighted. Finally, the full EMP will be presented in section 2.4.

2.1 Electrical

2.1.1 Main grid connection

In the paper, the MG can buy or sell energy from or to the main grid. Buying and selling time-dependent costs are considered. Lets note, p_{in}, p_{out} the input and output powers and the related instantaneous costs c_{in}, $c_{out} \in \mathbb{R}$. The main grid can be formulated as follow:

$$p_{in}(t), p_{out}(t) \in \mathbb{R}^{+} \qquad p_{mg}(t) \in \mathbb{R} \tag{1}$$

$$p_{mg}(t) = p_{in}(t) - p_{out}(t) \tag{2}$$

$$J_{mg} = \sum_{t} \left[c_{in}(t).p_{in}(t) + c_{out}(t).p_{out}(t) \right] .\delta t \tag{3}$$

If the instantaneous cost function is convex with respect to the power p_{mg}, *i.e.* when $c_{in}(t) \geqslant -c_{out}(t)$, selling and buying in the same time is impossible since the cost is to be minimize. Otherwise, to ensure not selling and buying energy in the same time, one can introduce a binary variable and additional

constraints such as

$$u_{mg} \in \{0\ ;1\} \qquad p_{mg}^{max}, p_{mg}^{min} \in \mathbb{R} \tag{4}$$

$$p_{in}(t) - u_{mg}(t).p_{mg}^{max} \leqslant 0 \tag{5}$$

$$p_{out}(t) + u_{mg}(t).p_{mg}^{min} \leqslant p_{mg}^{min} \tag{6}$$

2.1.2 Battery modelling

For an energetic context, the battery can be modelled by a constant charging and discharging maximal power with respect to the state of charge (SOC) [13,14]. If we consider charging and discharging efficiency η_c and η_d, one should consider a binary formulation of the following form:

$$e(t) \geqslant e_{min} \in \mathbb{R}^+ \qquad e(t) \leqslant e_{max} \tag{7}$$

$$e(0) = e_0 \qquad e(t_f) = e_f \tag{8}$$

$$p_c, p_d \in \mathbb{R}^+ \qquad u_b \in \{0\ ;1\} \tag{9}$$

$$p_c(t) - u_b(t).p_c^{max} \leqslant 0 \qquad p_c^{max} \in \mathbb{R}^+ \tag{10}$$

$$p_d(t) + u_b(t).p_d^{max} \leqslant p_d^{max} \qquad p_d^{max} \in \mathbb{R}^+ \tag{11}$$

$$\frac{\partial e(t)}{\partial t} = p_c(t).\eta_c - \frac{p_d(t)}{\eta_d} \tag{12}$$

This model is drastically simplified considering ideal efficiencies, and eqs. (9)–(12) can be replaced by the linear and continuous eqs. (13) and (14).

$$p_{bat}(t) \geqslant -p_d^{max} \qquad p_{bat}(t) \leqslant p_c^{max} \tag{13}$$

$$\frac{\partial e(t)}{\partial t} = p_{bat}(t) \tag{14}$$

In MG literature, we usually consider a battery reserve in order to prevent a possible disconnection of the main grid. For simplicity, and because the non-linear formulation does not consider it, we will not include it. It is also possible to add battery cost, depending on the charging and discharging powers or on SOC.

2.1.3 Generalities

The electrical sub-optimization problem can be seen as a classical unit commitment problem, where loads, DES and the grid connexion are the main components involved. In the MILP case, the unit commitment problem can be written as follows :

$$p_{pv}(t) + p_{mg}(t) + p_{de}(t) = p_{ex}(t) + p_h(t) + p_{bat}(t) + \widetilde{p_v}(t) + p_e(t) \tag{15}$$

$$p_h(t) \in [0\ ; p_h^{max}] \qquad p_{de}(t) \in \mathbb{R}^+ \qquad p_{ex}(t) \in \mathbb{R}^+ \tag{16}$$

where p_h is the heating electrical power, p_{pv} is the forecast power of the PV panels, $\widetilde{p_v}$ is the linear approximation of the ventilation power, and p_e is the electrical load demand.

Two positive decision variables are added to ensure the feasibility of eq. (15) in every configurations, the deficit power p_{de} and the excess power p_{ex}. Those variables are also included in the electric objective function, eq. (17) to penalise excess and deficit power. The full electrical objective is thus describes as:

$$J_{elec} = J_{mg} + \sum_t \left[M_{de}.p_{de}(t) + m_{ex}.p_{ex}(t)\right].\delta t \tag{17}$$

The positive weight are usually chosen such as $M_{de} \gg c_{in}$ and $m_{ex} \approx 0$.

Note that the continuous formulation shows some limits when it comes to different selling/buying costs or charging/discharging efficiency in eqs. (3) and (12).

2.2 Thermal

2.2.1 Thermal envelop

Both formulation, NLP and MILP are based on a linear model of the building structure and derives from a resistance-capacity network. It is usually described by a linear state-space system [15, 16]. It consist on a set of equality constraint to ensure heat flow and energy conservation. In the general case, a $n \in \mathbb{N}$ thermal-zone building involves n states $T_j(t)$ and n ideal heating inputs $p_h^j(t)$. We note $p_h(t) = \sum_j p_h^j(t)$ the total instantaneous heating power, where $j \in \{0, .., n\}$ denotes the thermal zone index. The thermal model also considers heat gain, such as occupancy, solar or electrical gains.

A general the temperature variation within the thermal-zones can be model by the following state-space system.

$$\dot{T}(t) = A.T(t) + B.U(t) \quad (18)$$

where A and B are fixed matrix, taking into account, resistance, capacity values and thermal network topology. $U(t)$ usually represents boundary conditions, such as a fixed external temperature, and the indoor heat gains and forced-air heater power.

2.2.2 Comfort assumptions

Comfort modelling is usually non-linear and discrete, between winter and summer period or between days and night. The simple incomfort cost expression has the same form than the electricity cost. In general, it can be formulated as follows:

$$J_{th} = \sum_t c_i(t).y(t).\delta t \quad (19)$$

$$y(t) \in S \quad (20)$$

where $c(t)$ and $y(t)$ represent a time-dependent discomfort cost and the discomfort variable. S describes a bounded convex set.

As an example, for discomfort modelling in winter period, one could constraint the discomfort to be positive for temperature under the reference temperature profile $T_r^j(t)$, where j denotes the thermal zone index, and null above it as follows:

$$y^j(t) \in \mathbb{R}^+ \quad (21)$$

$$y^j(t) \geqslant T_r^j(t) - T_{int}^j(t) \quad (22)$$

$$J_{th} = \sum_t \sum_j c_i(t).y^j(t).\delta t \quad (23)$$

2.3 Ventilation and Air Quality

In the paper, we consider ventilation system of the building. It is actually the key point of the NLP/MILP comparison and has an important impact on both thermal and air-quality phenomenons. As we consider a trade off objective function between cost-of-use and thermal comfort, ventilation control will also have a important impact on the electrical grid and thus, plays a central role in the system. Moreover, it presents non-linearity and non-convexity.

2.3.1 Linearisation of the ventilation power

For the non-linear continuous formulation, the ventilation power p_v is identified as a second order polynomial, eq. (24).

$$p_v(t) = f(Q_v) = \alpha_2.Q_v(t)^2 + \alpha_1.Q_v(t) + \alpha_0 \quad (24)$$

where Q_v si the ventilation air flow ($m^3.h^{-1}$), and α_0, $\alpha_1 \in \mathbb{R}$ and $\alpha_2 \in \mathbb{R}^+$ are constant values. Constructor or experimental data could be easily used to identify such behaviour. We propose here a piecewise linear approximation for the MILP formulation.

It is important to note that p_v is directly linked to the term p_{mg} by eq. (15). In other words, minimizing p_v is always equivalent to minimize the global objective function. Then, a linear approximation of $p_v(t)$, noted $\widetilde{p_v}(t)$ can be done by adding a set of inequalities.

$$n_{d2} \in \mathbb{N} \qquad k \in \{0\ ;1\ ;\ ..\ ;n_{d2}-1\} \tag{25}$$

$$\widetilde{p_v}(t) \leqslant \nu_1^k.Q_v(t) + \nu_0^k,\ \forall k \qquad \widetilde{p_v} \in \mathbb{R} \qquad Q_v \in \mathbb{R} \tag{26}$$

where the coefficients ν_1^k and ν_0^k are computed as follow :

$$\nu_1^k = f'(C^k) \qquad \nu_0^k = f(C^k) \tag{27}$$

The term C^k represents a set of linearisation points. This is a really light formulation. Note that it is possible with all non-linear convex function, differentiable on the set C^k. Eq. (26) can be improved in particular case to minimize the mean error of this approximation, but a general formulation is difficult. For non-convex function, one could use a SOS2 formulation as in eq. (31).

2.3.2 Approximation of the products x.y

In this paragraph, we propose a general linear approximation of the product $z = x.y$, where $x, y \in \mathbb{R}$ are continuous optimization variables. First we decouple the two variables by setting the substitution as in eq. (29).

$$x, y, z \in [0\ ;1] \tag{28}$$

$$a = \frac{1}{2}(x+y) \qquad b = \frac{1}{2}(x-y) \tag{29}$$

Note that $z = x.y = a^2 - b^2$. This formulation is still good for other decision variables limits. In order to lower the matrix range, and so the convergence quality, one could normalize the definition range of the variables.

For both terms, a^2 and b^2 we define a special ordered set of type 2 (SOS2) using the real valued decision variables w_a^i and w_b^i and the quantity break points A^i and B^i. For clarity, we explicit a binary formulation of the SOS2 for the linear approximation of the term a^2 in eqs. (30) and (31).

$$n_d \in \mathbb{N} \qquad i \in \{0\ ;..\ ;n_{d1}\} \qquad j \in \{0\ ;\ ..\ ;n_{d1}-1\} \tag{30}$$

$$\begin{cases} u_a^j, \in \{0\ ;1\} \\ w_a^i, \in [0\ ;1] \\ \sum_j u_a^j = 1 \\ u_a^j \leqslant w_a^j + w_a^{j+1} \\ a = \sum_i w_a^i.A^i \end{cases} \tag{31}$$

The priecewise approximation of both terms a^2 and b^2 is then straight forward knowing the weight w_a^i, w_b^i.

$$a^2 \approx \widetilde{z_a} = w_a^i.\left(A^i\right)^2 \qquad b^2 \approx \widetilde{z_b} = w_b^i.\left(B^i\right)^2 \tag{32}$$

Finally, approximation of z, noted $\widetilde{z}$, can be express as the difference between both approximations $\widetilde{z_a}$ and $\widetilde{z_b}$ as:

$$z \approx \widetilde{z} = \widetilde{z_a} - \widetilde{z_b} \tag{33}$$

2.3.3 Linearisation of heat flow

Thermal behaviour of ventilation system can vary from on technology to another. However, it is generally modelled as a non-linear heat flow input, with respect to the air flow Q_v, the inner and outer temperatures T_{ext}, T_{int}, an exchanger efficiency (for heat recovering ventilation) and air properties. The NL expressing of $q_v(t)$ is described in eq. (34).

$$q_v(t) = \rho.c_p.(1-\eta_v).Q_v(t).(T_{int}(t) - T_{ext}(t)) \quad (34)$$

The product $Q_v(t).T_{int}(t)$ is approximated using the method explained in 2.3.2. This linearisation leads to the introduction of the approximated heat flow noted $\widetilde{q_v}$.

2.3.4 The air quality model

Control of ventilation is usually a trade-off between air quality constraints and thermal comfort. Thus, an air quality model is needed. In this article, we only consider CO_2 concentration in air quality model. Thermal discomfort is to be minimized whereas air quality, *i.e* CO_2 concentration is constrained to a low level since the link between air quality and comfort is not straight forward , see eq. (35). The non-linear conservation equation of the gas takes into account, air flow rate Q_v and the occupancy N_p, see eq. (37).

$$C_{co2}(t) \in \left[C_{co2}^{air}\ ; C_{co2}^{max}\right] \quad (35)$$

$$Q_v(t) \in \left[Q_v^{min}\ ; Q_v^{max}\right] \quad (36)$$

$$V.\frac{\partial C_{co2}(t)}{\partial t} = N_p(t).Q_p.C_{co2}^p - Q_v(t).(C_{co2}(t) - C_{co2}^{air}) \quad (37)$$

where V, Q_p, C_{co2}^p and C_{co2}^{air} denote respectively the volume of the room, the expired air flow by occupant, the mean expired CO_2 concentration by occupant and the outside CO_2 concentration. The product $Q_v(t).C_{co2}(t)$ in eq. (37) is linearised using the method explained in 2.3.2 and leads to the linear approximation of the CO_2 concentration noted $\widetilde{C_{co2}}(t)$.

2.4 Full Optimization Problem

Both continuous non-linear, and mixed integer linear formulations consider the same objective function, *i.e.* no approximation or linearisation are needed. It sums the electricity cost and the thermal discomfort cost (*c.f.* eqs. (17) and (19)).

2.4.1 Non-linear formulation

The continuous non-linear formulation includes all the constraints related to the main-grid, batteries, the thermal envelop and the ventilation system (*c.f.* eqs. (1)–(3), (7), (8), (13)–(20), (24) and (34)–(37)).

2.4.2 Mixed-Integer Linear Formulation

The mixed-integer linear programming includes all the constraints related to the main-grid, batteries, the thermal envelop and the piecewise approximations of the ventilation system (*c.f.* eqs. (1)–(12), (15)–(20) and (25)–(27)). Note that approximations are not explicitly develop every time for consistency matters. Piecewise linear approximations of p_v, q_v and C_{co2} are all based on the method developed in section 2.3.2 and eqs. (28)–(32).

3. Computational Experiment

In this section we propose a simple test case for an actual comparison between NLP and MILP formulations. We thus propose a fixed architecture of the microgrid, a thermal envelop, common boundary conditions and sizing.

For the MILP approach, simulation of the system and EM optimization are solved in the same optimisation loop, using Gurobi[1] and a step time dt_L. In the other hand, simulation is considered as and internal loop in the EM optimisation for the NLP formulation. As a result, two time steps are used: one for the simulation (usually $10min$) and one for the EM optimization, $dt_{NL} = 1h$.

3.1 Boundary conditions

The boundary condition consist of fixed time-dependent profiles :

- weather forecasts *i.e.* the outdoor temperature and the radiance which correspond to a winter day in Europe,
- the electricity price, which is assumed to be piecewise constant (see fig. 2a),

[1] `http://www.gurobi.com`

- the PV power generation, based on weather forecasts,
- occupancy profiles, *i.e.* presence, electricity use, thermal reference and CO_2 concentration upper limit ($CO_2^{max} = 1000\ ppm$).

3.2 MG Configuration

The electrical configuration of the microgrid involves a connexion to the main grid without selling option (*i.e.* $c_{out} = 0$), $24m^2$ PV panel, one battery pack with a capacity of $10kW.h$ and the heating and ventilation system. Initial values and parameters' description can be found in table 3.

3.3 Single-zone thermal envelop

In this numerical experimentation, the thermal envelop involves one zone and is modelled by a RC network of the 5th order. It incorporates 4 walls, each described by one capacity and two resistance, one inner capacity C_{air}, two resistances representing infiltrations and ventilation and one heat source representing the heating power, solar, electric and occupancy inputs, noted p_h, p_e, p_{sol} and p_{occ}. The identification of the parameters has been done using EnergyPlus as a reference [17]. Network topology and identified values are respectively available in fig. 1 and table 1.

Capacity	Value ($\times 10^6$)	Resistance	Value
C_{air}	3.7473	R_1	1.0400×10^{-2}
C_1	3.8832	R_2	7.8945×10^{-3}
C_2	2.3333	R_3	4.1700×10^{-3}
C_3	3.0388	R_4	1.7195×10^{-1}
C_4	8.1109	R_5	1.6600×10^{-1}
		R_6	6.7131×10^{-2}
		R_7	1.3500×10^{-2}
		R_8	1.2774×10^{-1}
		R_9	2.2000×10^{-3}

Table 1. Capacities and thermal resistances values identified using EnergyPlus

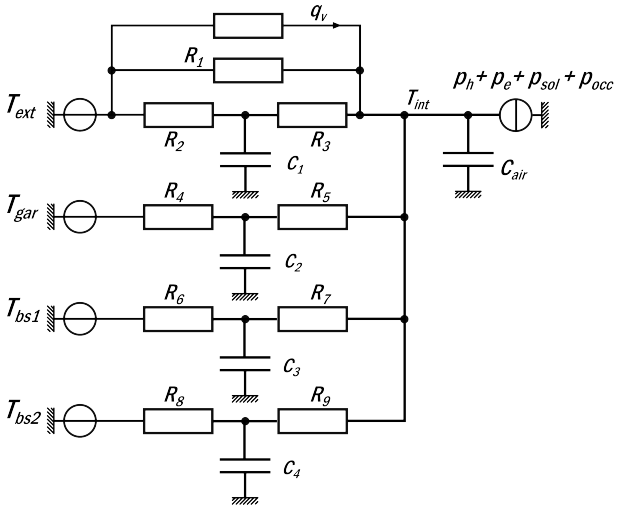

Figure 1. Thermal Envelop

4. Results

This section consists of a comparison of both NLP, MILP approaches applied to the use case presented in 3.. It includes a modelling and optimization performances comparison. Main figures can be found in table 2 and the following paragraphs will refer to it.

4.1 Modelling comparison

NLP formulation is developed within the CADES framework [2], providing automatic differentiation of the model. This ensure an easy modelling stage using a combination of SML, *i.e.* the CADES language and

[2] `http://www.vesta-system.fr/fr/produits/cades/vesta-cades.html`

Table 2. Performances comparison

formulation	*time step*	*lines of code*	*continuous/binary variables*	*nbr. constraints / matrix size**	*computation time (s)*	*elec. cost (€)*
NLP	(10 *min*, 1 *h*)	547	72/0	72	2.00	5.212
	1 *h*	3 859	554/111	660/665/2256	0.73	5.456
MILP	30 *min*	7 607	1 083/231	1358/1314/4615	8.91	4.876
	20 *min*	11 441	1 617/346	2032/1963/6912	43.71	4.737

*nbr. of rows/nbr. of columns/nbr. of nonzeros

C++ functions. About 547 lines of codes are dedicated to the modelling (the solver is not included) for about 72 optimization variables and 72 constraints, see table 2. Indeed, dynamic constraints, *e.g.* the thermal state system eq. (18), are solved during an internal loop and are not considered by the global NLP solver.

For a one-hour time step, the MILP formulation consists of 3 859 lines in a LP language, which can be drastically minimized using a high level modelling language, such as AMPL, GAMS or Pyomo. It includes 660 constraints, 554 continuous and 111 binary variables, see table 2.

4.2 Optimization results and performances

This paragraph aims to compare optimization results, *i.e* convergence proprieties and speed. Computation time and optimal electrical costs are detailed in table 2. NLP is soled using a sequential quadratic programming (SQP) solver [18] within the CADES framework, whereas the MILP is solved using bunch and bound and dual simplex algorithms within Gurobi.

Most of time-dependant quantities are presented in fig. 2. Results are plotted for a discomfort cost related to the cost of electricity where $\frac{c_i(t)}{c_{in}(t)} = 0.8$, and leads to a null discomfort cost for each case, see fig. 2d.

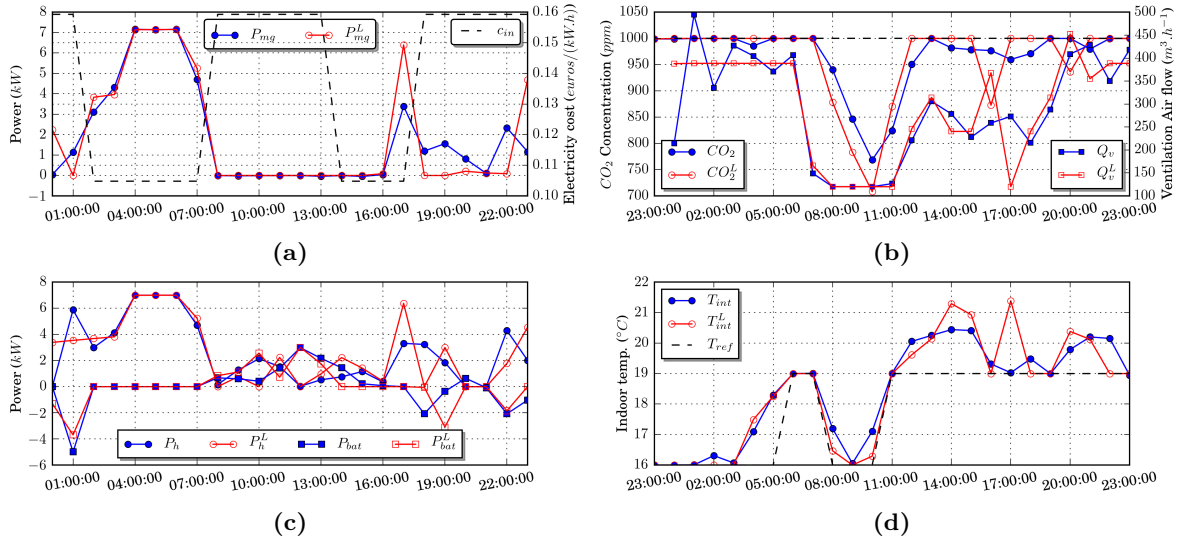

Figure 2. Optimal energy management results - a comparative study between NLP and MILP (noted X^L) formulations. **(a)** Main grid power and buying price, **(b)** CO_2 concentration (ppm) and ventilation air-flow ($m^3.h^{-1}$), (c) heating and battery pack power (kW) and **(d)** Indoor and reference temperatures ($^\circ C$).

Note that several optimal solutions are likely because of the multiple control variables, thermal and electrical storage capacities. One can see the global agreement between both results, especially from $23h$ to $15h$. The indoor temperature profiles gently follows the references, taking into account dynamics of the model. Between 14 and $15h$, thermal storage of the building is used during the low-cost period. We then note small differencies between $16h$ and $17h$ for the air quality and ventilation control (see fig. 2b) and at $17h$ for the thermal control (see figs. 2b and 2c). Those differences could be explains, by several optimal solutions or by small differences between NLP formulation and linear approximations.

In terms of convergence quality, we note a better accuracy for the MILP formulation. Between 8 and $15h$, P^L_{mg} is lower than 1×10^{-12}, whereas P_{mg} vary between -40 and $-3W$ which is irrelevant in this context. Nevertheless, optimal electrical costs are coherent and tend to show that both formulations are relevant for the EM optimization.

Computation time are about the same for one hour time step, with an advantage for the MILP formulation

as expected. However, Results for smaller time-step tends to show some scalability issues due to the high number of binary variables (table 2).

5. Conclusion and Perspective

Acknowledgement

The research leading to these results has received funding from the People Programme (Marie Curie Actions) of the European Union's Seventh Framework Programme FP7/2007-2013/ under project ELECON - Electricity Consumption Analysis to Promote Energy Efficiency Considering Demand Response and Non-technical Losses, REA grant agreement No 318912.

Notations

Notation, short description and units of all quantities are available in table 3.

REFERENCES

[1] A. A. Khan, S. Razzaq, A. Khan, F. Khursheed, *et al.*, "Hemss and enabled demand response in electricity market: an overview," *Renewable and Sustainable Energy Reviews*, vol. 42, pp. 773–785, 2015.

[2] Y. Lu, S. Wang, and K. Shan, "Design optimization and optimal control of grid-connected and standalone nearly/net zero energy buildings," *Applied Energy*, vol. 155, pp. 463–477, 2015.

[3] F. Eddy, H. B. Gooi, and S. X. Chen, "Multi-agent system for distributed management of microgrids," *Power Systems, IEEE Transactions on*, vol. 30, no. 1, pp. 24–34, 2015.

[4] F. Shariatzadeh, P. Mandal, and A. K. Srivastava, "Demand response for sustainable energy systems: A review, application and implementation strategy," *Renewable and Sustainable Energy Reviews*, vol. 45, pp. 343–350, 2015.

[5] Z. Li, G. Yang, C. Pan, and Q. Gong, "Demand response based on dynamic electricity price and energy consumption of residential house," in *Chinese Automation Congress (CAC), 2015*, pp. 1361–1365, IEEE, 2015.

[6] S. Parhizi, H. Lotfi, A. Khodaei, and S. Bahramirad, "State of the art in research on microgrids: a review," *Access, IEEE*, vol. 3, pp. 890–925, 2015.

[7] C. Gamarra and J. M. Guerrero, "Computational optimization techniques applied to microgrids planning: a review," *Renewable and Sustainable Energy Reviews*, vol. 48, pp. 413–424, 2015.

[8] P. Palensky and D. Dietrich, "Demand side management: Demand response, intelligent energy systems, and smart loads," *IEEE transactions on industrial informatics*, vol. 7, no. 3, pp. 381–388, 2011.

[9] S. Vandael, B. Claessens, M. Hommelberg, T. Holvoet, and G. Deconinck, "A scalable three-step approach for demand side management of plug-in hybrid vehicles," *IEEE Transactions on Smart Grid*, vol. 4, pp. 720–728, June 2013.

[10] D. Patteeuw, K. Bruninx, A. Arteconi, E. Delarue, W. D'haeseleer, and L. Helsen, "Integrated modeling of active demand response with electric heating systems coupled to thermal energy storage systems," *Applied Energy*, vol. 151, pp. 306–319, 2015.

[11] A. Arteconi, D. Patteeuw, K. Bruninx, E. Delarue, W. D'haeseleer, and L. Helsen, "Active demand response with electric heating systems: impact of market penetration," *Applied Energy*, vol. 177, pp. 636–648, 2016.

[12] Q. D. Ngo, Y. Hadj-Said, S. Ploix, B. Parisse, and U. Maulik, "Toward the automation of model transformation for optimized building energy management," in *Clean Energy and Technology (CEAT), 2013 IEEE Conference on*, pp. 336–341, IEEE, 2013.

[13] D. Tenfen, E. C. Finardi, B. Delinchant, and F. Wurtz, "Lithium-ion battery modelling for the energy management problem of microgrids," *IET Generation, Transmission & Distribution*, vol. 10, no. 3, pp. 576–584, 2016.

Not.	Description	Unit
○ p_{in}	*MG input power*	kW
○ p_{out}	*MG output power*	kW
△ c_{in}	*input instantaneous cost*	€$.h^{-1}$
△ c_{out}	*input instantaneous cost*	€$.h^{-1}$
○ p_{mg}	*MG power*	kW
▫ p_{mg}^{max}	*maximal MG power*	25 kW
▫ p_{mg}^{min}	*minimal MG power*	25 kW
○ J_{mg}	*total cost of the MG*	€
◇ u_{mg}	*on/off binary variable*	-
○ e	*battery SOC*	$kW.h$
▫ e_{min}	*minimal SOC*	0.5 $kW.h$
▫ e_{max}	*maximal SOC*	10 $kW.h$
▫ e_0	*initial SOC*	5 $kW.h$
▫ e_f	*final SOC*	50 $kW.h$
○ p_{bat}	*battery power*	kW
• p_c	*battery charging power*	kW
▫ p_c^{max}	*maximal charging power*	5 kW
• p_d	*battery discharging power*	kW
▫ p_d^{max}	*maximal discharging power*	5 kW
◇ u_b	*on/off binary variable*	-
△ p_{pv}	*photovoltaic generated power*	kW
○ p_{de}	*deficit power*	kW
○ p_{ex}	*excess power*	kW
• p_h	*heating power*	kW
▫ p_h^{max}	*maximal heating power*	7 kW
○ p_v	*ventilation electric power*	kW
○ $\widetilde{p_v}$	*approximation of* p_v	kW
△ p_e	*elec. load demand*	kW
△ p_{pv}	*PV generation*	kW
○ s^+	*positive discomfort*	$°C$
○ s^-	*negative discomfort*	$°C$
○ q_v	*ventilation heat flow*	$m^3.s^{-1}$
△ T_r	*internal reference*	$°C$
▫ η_v	*heat recovering efficiency*	0 -
▫ rho	*air density*	1.225 $kg.m^{-3}$
○ T_{int}	*internal temperature*	$°C$
▫ c_p	*air heat capacity*	$2.775e^{-3}$ $kW.h/kg/K$
△ c_i^+	*positive deviation cost*	€$.h^{-1}$
△ c_i^-	*negative deviation cost*	€$.h^{-1}$
○ J_{th}	*thermal discomfort cost*	€
▫ Q_p	*respiration air flow*	$4e^4$ $m^3.h^{-1}$
○ Q_v	*ventilation air flow*	$m^3.h^{-1}$
▫ Q_v^{min}	*min. ventilation air flow*	120 $m^3.h^{-1}$
▫ Q_v^{max}	*max. ventilation air flow*	1000 $m^3.h^{-1}$
○ C_{co2}	*CO_2 concentration*	ppm
▫ C_{co2}^{max}	*max. CO_2 concentration*	$1e^4$ ppm
▫ C_{co2}^{air}	*external CO_2 concentration*	400 ppm
▫ C_{co2}^{p}	*expired CO_2 concentration*	$4e^5$ ppm
△ N_p	*occupancy*	-
▫ V	*volume of the room*	650.45 m^3

○ : optimisation variable, ▫ : fixed scalar, △ : given input profile, • : decision variable

Table 3. Notations

[14] D. Tenfen and E. C. Finardi, “A mixed integer linear programming model for the energy management

problem of microgrids," *Electric Power Systems Research*, vol. 122, pp. 19–28, 2015.

[15] E. M. Burger, H. E. Perez, and S. J. Moura, "Piecewise linear thermal model and recursive parameter estimation of a residential heating system," 2016.

[16] S. Goyal and P. Barooah, "A method for model-reduction of non-linear thermal dynamics of multi-zone buildings," *Energy and Buildings*, vol. 47, pp. 332–340, 2012.

[17] D. B. Crawley, L. K. Lawrie, F. C. Winkelmann, W. F. Buhl, Y. J. Huang, C. O. Pedersen, R. K. Strand, R. J. Liesen, D. E. Fisher, M. J. Witte, *et al.*, "Energyplus: creating a new-generation building energy simulation program," *Energy and buildings*, vol. 33, no. 4, pp. 319–331, 2001.

[18] P. Gill, W. Murray, and M. Saunders, "Large-scale sqp methods and their application in trajectory optimization," in *Computational Optimal Control* (R. Bulirsch and D. Kraft, eds.), vol. 115 of *ISNM International Series of Numerical Mathematics*, pp. 29–42, Birkhäuser Basel, 1994.